

# Design of Next-Generation Mid-infrared Multimaterial Fiber Optics

Xiaoyu Ji<sup>\*1</sup>, Ryan L. Page<sup>1,#</sup>, and Venkatraman Gopalan<sup>1</sup>

<sup>1</sup>Department of Materials Science and Engineering, Pennsylvania State University, University Park, PA 16802, USA

<sup>#</sup>Present address: Department of Materials Science and Engineering, Cornell University, Ithaca, NY 14850, USA

<sup>\*</sup>Corresponding author: xuj104@psu.edu

**Abstract:** Optical fibers that can deliver mid-infrared light in a wide wavelength range are in high demand due to their significant potentials in sensors, chemical imaging, optoelectronics and nonlinear optics applications. Semiconductors such as Ge, ZnSe and Si are good infrared-transparent materials. Using these materials as the fiber cores and silica as the fiber cladding offers opportunities in realizing next-generation mid-infrared multimaterial fiber optics. Optical propagation losses of such structures are simulated using COMSOL Multiphysics® for different wavelengths and fiber geometries. The optimum operation wavelength ranges for different fiber geometries are found and strategies to introduce additional interfacial layers are demonstrated to be effective in further reducing the optical losses. Initial experimental results show that such optical fibers have potential for mid-infrared waveguiding, and the simulation results in this work provides guidance for realizing better performance in practice.

**Keywords:** Semiconductor optical fiber, mid-infrared, materials design

## 1. Introduction

The mid-infrared ( $\lambda \sim 3\text{-}8\mu\text{m}$ ) and long-infrared ( $\lambda \sim 8\text{-}15\mu\text{m}$ ) wavelength ranges are of tremendous importance for materials research as well as sensor technologies due to the vibrational resonances that yield unique chemical signatures of materials. The wavelength range is also finding increasing importance in sensors, night vision, automotive and airline industry, non-destructive testing and process monitoring, free-space communications, biology and health care such as in endoscopy and imaging. Semiconductor optical fibers are an emerging platform for optoelectronics, photonics, and imaging. The wide infrared transmission window, high refractive index ( $n \sim 4$ ), and high carrier mobility of germanium (Ge) make it a very attractive material for electronic and infrared imaging

applications. Specific applications of Ge fiber waveguides include the development of mid-infrared endoscopes and photodetectors. Here, we try to investigate and design small core diameter Ge core based optical fibers with low optical loss at mid-infrared.

### 1.1 Semiconductor Optical Fibers

Semiconductor optical fibers are an important class of infrared fibers<sup>[1]</sup>. Many important semiconductors, such as Ge, ZnSe and Si, are transparent to infrared due to their small extinction coefficients in that wavelength range. The optical constants ( $n$  and  $k$ )<sup>[2]</sup> for several important semiconductors together with fused silica (conventional material for optical fibers) are plotted in Figure 1. Among these, Ge and ZnSe have extremely low extinction coefficients from 2-9  $\mu\text{m}$  such that they cannot be experimentally measured, showing great potential as mid-infrared waveguiding medium.

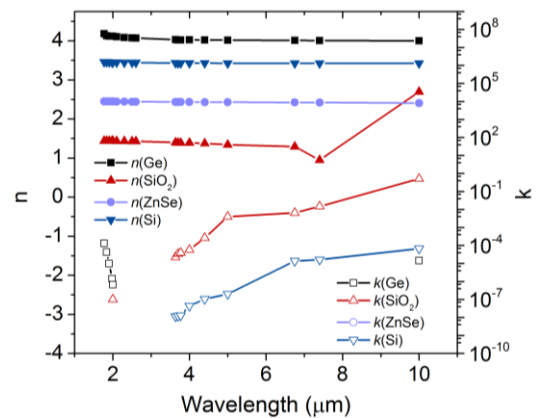


**Figure 1.** Optical constants ( $n$  and  $k$ ) for Ge, silica, ZnSe and Si adapted from Ref. 2.

Techniques to fabricate such semiconductor core/glass cladding step-index fibers include high pressure chemical vapor deposition (HPCVD)<sup>[3-5]</sup>, molten-core drawing<sup>[6,7]</sup> and pressure-assisted filling<sup>[8]</sup>. A schematic of such fibers is depicted in Figure 2.

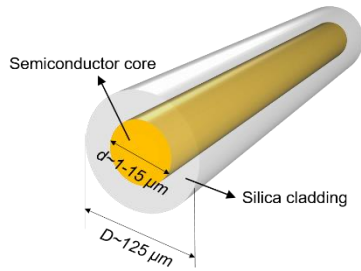


**Figure 2.** Schematic of a semiconductor core optical fiber.

### 1.2 Opportunities for Modeling

Although Ge core optical fibers have been realized experimentally, the optical transmission/loss spectrum is less studied. Because the light transmission behavior of a material in a waveguide geometry is usually different from that in bulk<sup>[9]</sup>, therefore it is worth to study separately. Additionally, experiments are high-cost and time-consuming, therefore before doing experiments, simulation can provide a guidance and obtain the optimum operation wavelength range for fibers at different geometries.

## 2. Use of COMSOL Multiphysics® Software

Radio Frequency Module of COMSOL Multiphysics® 5.2 has been used for the mode analysis and optical loss simulations. Once the geometries are set, refractive indices (real part and imaginary part) are given to the core and cladding materials at certain wavelength. Triangular meshing element was used. The governing equation in this problem is the Helmholtz equation for the electric field:

$$\nabla \times (\nabla \times E) - k_0^2 n^2 E = 0$$

The boundary condition is that the electric field is zero along the outside of the cladding. The effective indices are obtained from mode analysis and the fundamental HE<sub>11</sub> modes are found by searching the largest index from the various modes in the multimodal fibers. After the mode analysis, optical attenuations at different wavelengths are calculated.

## 3. Results and Discussion

The electric field distribution of a characteristic HE<sub>11</sub> mode confined and guided inside a 6 μm core diameter Ge fiber is shown in Figure 3. In order to determine the optimum fiber geometry and the fiber operation wavelength range, the propagation attenuation of the HE<sub>11</sub> mode guided inside the Ge core/silica cladding fibers are then simulated as a function of wavelength and core diameters, as is shown in Figure 4. It can be noticed that there exists a low-loss window from 2-4.2 μm, and the loss increases at longer wavelength because 1) the evanescent wave extends more into the cladding region (Figure 5) and 2) the extinction coefficient (*k*) for silica also increases at longer wavelength. Also, the smaller the core diameter is, the larger the loss associated with this effect.

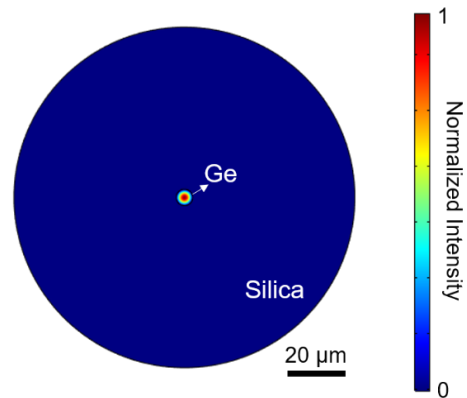


**Figure 3.** A characteristic HE<sub>11</sub> mode confined and guided inside a 6 μm core diameter Ge fiber

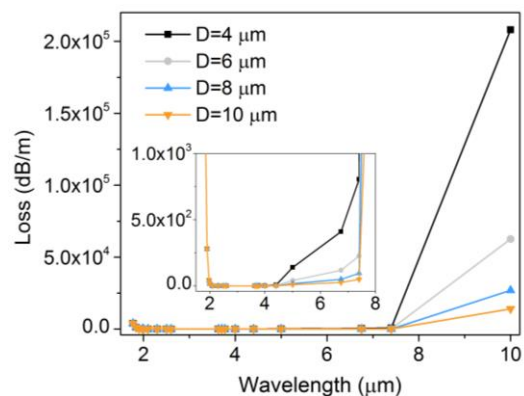


**Figure 4.** Optical loss simulated for Ge core/silica cladding fibers as a function of wavelength and core diameters. The inset is a zoomed-in figure showing the loss value difference beyond 4 μm for different core diameters.

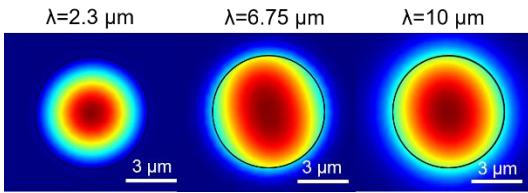


**Figure 5.** The electric field intensity distribution of  $HE_{11}$  mode in a  $6 \mu\text{m}$  Ge core fiber at different wavelengths, showing that the field extends more to the cladding at longer wavelength. This results in the higher optical losses at longer wavelength.

In order to further reduce the optical loss at longer wavelength so that we can achieve wider high-transmission window, an additional layer of materials between the Ge and silica is needed. And this interfacial material needs to have smaller refractive indices ( $n$ ) than that of Ge and smaller extinction coefficients ( $k$ ) than that of silica over a wide wavelength range. ZnSe and Si are good candidates. The characteristic  $HE_{11}$  mode confined and guided inside a  $6 \mu\text{m}$  core diameter Ge/Si and Ge/ZnSe structure fiber is shown in Figure 6. We simulated the optical loss as a function of wavelength of a  $6 \mu\text{m}$  diameter core silica fiber capillary, which has an either Ge ( $4 \mu\text{m}$ )/ZnSe ( $2 \mu\text{m}$ ) or Ge ( $4 \mu\text{m}$ )/Si ( $2 \mu\text{m}$ ) core. The result is shown in Figure 7. The effect of introducing the additional interfacial layer is significant in terms of reducing the optical propagation losses, especially at longer wavelengths. It is usually easier to achieve single mode guidance with a smaller core diameter fiber, so by introducing these interfacial layer, one doesn't need to sacrifice the core diameter to obtain low optical loss. Additionally, it can be seen that ZnSe has a more significant effect in reducing the loss, because the refractive index difference between Ge and ZnSe is larger comparing with Ge and Si, so that light can be better confined inside Ge (Figure 8). But smaller refractive index difference relatively reduce the constraint of a small core diameter for single mode guidance.

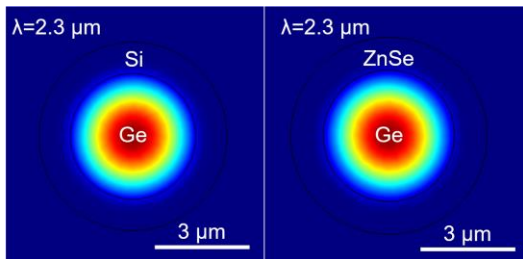


**Figure 6.** The characteristic  $HE_{11}$  mode confined and guided inside a  $6 \mu\text{m}$  core diameter Ge/Si and Ge/ZnSe structure fiber.

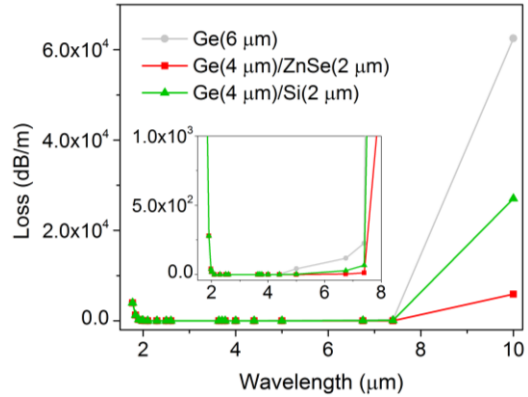


**Figure 7.** Optical loss simulated for Ge core/silica cladding fibers and for Ge/ZnSe core and Ge/Si core fibers as a function of wavelength. The inset is a zoomed-in figure showing the loss value difference beyond  $4 \mu\text{m}$  for different core materials.

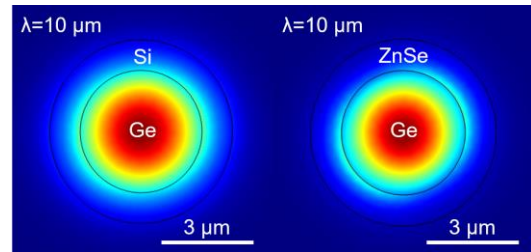


**Figure 8.** The intensity distribution of  $HE_{11}$  mode for Ge/Si and Ge/ZnSe core structures at wavelength of  $10 \mu\text{m}$ . The Ge/ZnSe structure confines light to the Ge region better, resulting in less optical loss.

We calculated the single mode guidance requirement for the Ge core diameter for both cases of using ZnSe and Si as the interfacial layer, and it can be seen from Figure 9 that Ge/ZnSe structure indeed requires a smaller Ge core diameter to achieve single mode guidance.

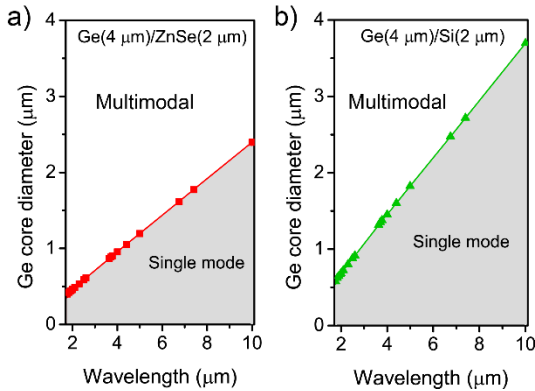


**Figure 9.** Ge core diameter requirements for the a) Ge/ZnSe and b) Ge/Si structures. The gray areas indicate single mode guidance conditions.

#### 4. Experimental Realization

In experiment, we have realized 6  $\mu\text{m}$  core diameter single crystal Ge core optical fibers with low optical losses using HPCVD method with post laser-annealing<sup>[10]</sup>. We are exploring the fabrication of Ge/ZnSe and Ge/Si structures and will report in the future.

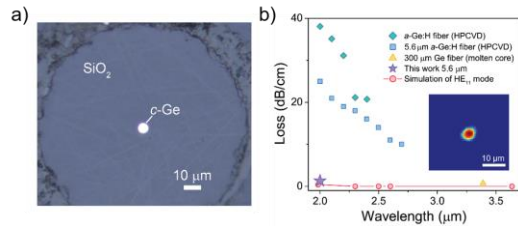


**Figure 10.** Experimental results of Ge core optical fiber. a) Optical micrograph. 2) Loss measurement.

#### 5. Conclusions

We have investigated the design of next-generation mid-infrared fiber optics based on germanium core optical fibers. Parameters such as wavelength, core diameters and interfacial layer materials are varied to optimize the fiber performances. These fibers may find applications in future spectroscopic imaging endoscopes<sup>[11]</sup>.

#### 6. References

[1] G. Tao, H. Ebdorff-Heidepriem, A. M. Stolyarov, S. Danto, J. V. Badding, Y. Fink, J. Ballato, A. F. Abouraddy, *Adv. Opt. Photonics* **2015**, 7, 379.

[2] E. D. Palik, *Handbook of Optical Constants of Solids, Volume 1*, Academic Press, **1985**.

[3] P. J. A. Sazio, A. Amezcua-Correa, C. E. Finlayson, J. R. Hayes, T. J. Scheidemantel, N. F. Baril, B. R. Jackson, D.-J. Won, F. Zhang, E. R. Margine, V. Gopalan, V. H. Crespi, J. V. Badding, *Science* **2006**, 311, 1583.

[4] S. Chaudhuri, J. R. Sparks, X. Ji, M. Krishnamurthi, L. Shen, N. Healy, A. C. Peacock, V. Gopalan, J. V. Badding, *ACS Photonics* **2016**, DOI 10.1021/acsphotonics.5b00434.

[5] J. R. Sparks, R. He, N. Healy, M. Krishnamurthi, A. C. Peacock, P. J. A. Sazio, V. Gopalan, J. V. Badding, *Adv. Mater.* **2011**, 23, 1647.

[6] J. Ballato, T. Hawkins, P. Foy, R. Stolen, B. Kokuoz, M. Ellison, C. McMillen, J. Reppert, A. M. Rao, M. Daw, S. R. Sharma, R. Shori, O. Stafsudd, R. R. Rice, D. R. Powers, *Opt. Express* **2008**, 16, 18675.

[7] J. Ballato, T. Hawkins, P. Foy, B. Yazgan-Kokuoz, R. Stolen, C. McMillen, N. K. Hon, B. Jalali, R. Rice, *Opt. Express* **2009**, 17, 8029.

[8] H. K. Tyagi, M. A. Schmidt, L. Prill Sempere, P. S. Russell, *Opt. Express* **2008**, 16, 17227.

[9] S. O. Kasap, *Optoelectronics and Photonics: Principles and Practices*, Prentice Hall, Upper Saddle River, NJ, **2001**.

[10] X. Ji, R. Page, S. Chaudhuri, W. Liu, S.-Y. Yu, S. E. Mohny, J. Badding, V. Gopalan, *Adv. Opt. Mater.* **2016**, in press, DOI 10.1002/adom.201600592.

[11] X. Ji, B. Zhang, M. Krishnamurthi, J. Badding, V. Gopalan, *Opt. Express* **2014**, 22, 28459.

#### 7. Acknowledgement

We acknowledge funding from the Penn State Materials Research Science and Engineering Center for Nanoscale Science, Grant No. DMR 1420620 and funding from National Science Foundation Grant No. DMR 1460920 for Research Experiences for Undergraduates (REU).